Systematic Analysis of Crosstalk Noise in Folded-Torus-Based Optical Networks-on-Chip

Mahdi Nikdast, *Student Member, IEEE,* Jiang Xu, *Member, IEEE,* Xiaowen Wu, *Student Member, IEEE,* Wei Zhang, *Member, IEEE,* Yaoyao Ye, *Student Member, IEEE,* Xuan Wang, *Student Member, IEEE,* Zhehui Wang, *Student Member, IEEE,* and Zhe Wang

***Abstract*—Photonic devices are widely used in optical networks-on-chip (ONoCs) and suffer from crosstalk noise. The accumulative crosstalk noise in large scale ONoCs diminishes the signal-to-noise ratio (SNR), causes severe performance degradation, and constrains the network scalability. For the first time, this paper systematically analyzes and models the worst-case crosstalk noise and SNR in folded-torus-based ONoCs. Formal analytical models for the worst-case crosstalk noise and SNR are presented. The crosstalk noise analysis is hierarchically performed at the basic photonic device level, then at the optical router level, and finally at the network level. We consider a general 5×5 optical router model to enable crosstalk noise and SNR analyses in folded-torus-based ONoCs using an arbitrary 5×5 optical router. Using the general optical router model, the worst-case SNR link candidates, which restrict the network scalability, are found. Also, we present a novel crosstalk noise and loss analysis platform, called CLAP, which can analyze the crosstalk noise and SNR of arbitrary ONoCs. Case studies of optimized crossbar and Crux optical routers using recent photonic device parameters are presented. Moreover, we compare the worst-case crosstalk noise and SNR in folded-torus-based and mesh-based ONoCs using optimized crossbar and Crux optical routers. The quantitative simulation results show the critical behavior of crosstalk noise in large scale ONoCs. For example, in folded-torus-based ONoCs using the Crux optical router, the noise power exceeds the signal power for network sizes larger than 12×12; when the network size is 20×20 and the injection signal power equals 0 dBm, the signal power and noise power are −9.4 dBm and −6.1 dBm, respectively.**

***Index Terms*—Folded-torus-based optical networks-on-chip (ONoCs), ONoCs, optical crosstalk noise, optical losses, signal-to-noise ratio (SNR).**

I. Introduction

THE NETWORK-ON-CHIP (NoC), as a new architectural trend, can enhance the bandwidth of metallic interconnects. However, as the number of possible integrated processing cores on a single die continues to increase, metallic interconnects are not able to satisfy the bandwidth and latency requirements within the package power budget. Furthermore, International Technology Roadmap for Semiconductors has predicted that the interconnects in multiprocessor systems-on-chip (MPSoCs) will become a serious issue in the near future [1]. On the other hand, studies have shown some advantages of optical networks-on-chip (ONoCs) as a proper substitute for electronic NoCs in MPSoCs. ONoCs benefit from considerably higher bandwidth, lower power dissipation, and lower latency [2]. Significant developments in optical devices have made optical on-chip routers and silicon-based optical waveguides possible [3], [4].

Crosstalk noise is a major drawback of the silicon waveguide crossings and microresonator-based photonic switching elements widely used in constructing ONoCs. Crosstalk noise is the result of undesirable mode coupling in optical signals. Although it is small at the device level, the crosstalk noise accumulates in large scale ONoCs, causes severe performance degradation and damage to the signal-to-noise ratio (SNR) in the network, and also constrains the scalability of the ONoCs. Vaez and Lea [5] indicated that the crosstalk noise is an intrinsic issue in directional-coupler-based optical networks and Xie *et al.* [6] showed the serious critical behavior of the crosstalk noise in mesh-based ONoCs. In the latter work, it was proved that the worst-case SNR link is not the longest optical link, which suffers from the highest power loss in the network. Therefore, it is vital to analyze the worst-case crosstalk noise and SNR in ONoCs. Xie *et al.* [6] also indicated that the power loss and crosstalk noise caused by the waveguide crossings play an important role in the network performance degradation. Some research works have tried to improve the waveguide crossings. Chen *et al.* [7] presented multimode interference (MMI)-based wire waveguide crossings, instead of conventional plain waveguide crossings, for the merits of low loss and low crosstalk. Chen *et al.* [8] introduced a design technique for a compact 5426 nm×5426 nm waveguide crossing by using a 90deg MMI based waveguide crossing sandwiched by four identical miniaturized tapers and improved the insertion loss and the crosstalk noise to −0.21 dB and −44.4 dB at a wavelength of 1550 nm. Li *et al.* demonstrated metal-free integrated elliptical reflectors for waveguide turnings and crossings. By employing four symmetric, identical elliptical reflectors sharing an intermediate beam focused

Manuscript received October 31, 2012; revised March 16, 2013 and September 17, 2013; accepted October 8, 2013. Date of current version February 14, 2014. This work was supported by DAG11EG05S. This paper was recommended by Associate Editor R. Marculescu.

M. Nikdast, J. Xu, X. Wu, W. Zhang, Y. Ye, X. Wang, Zhehui Wang, and Zhe Wang are with the Department of Electronic and Computer Engineering, Hong Kong University of Science and Technology, Clear Water Bay, Hong Kong (e-mail: mnikdast@ust.hk; jiang.xu@ust.hk; wxxaf@ust.hk; eeweiz@ust.hk; yeyaoyao@ust.hk; eexwang@ust.hk; zhehui@ust.hk; zwangag@ust.hk).

Color versions of one or more of the figures in this paper are available online at http://ieeexplore.ieee.org.

Digital Object Identifier 10.1109/TCAD.2013.2288676

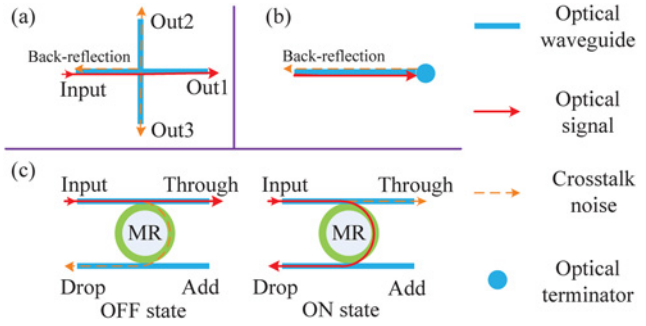

Fig. 1. (a) Waveguide crossing. (b) Optical terminator. (c) Parallel switching element.

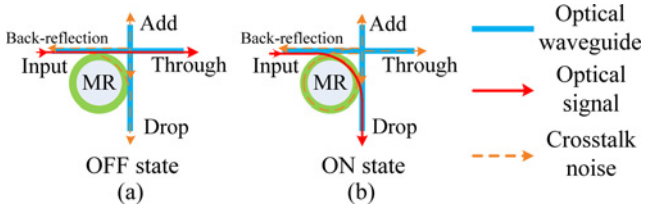

Fig. 2. Crossing switching element in the (a) OFF state and (b) ON state.

region in a direct waveguide crossing, crosstalk noise smaller than −30 dB and high transmission were achieved [9]. An ultracompact waveguide crossing with negligible crosstalk noise and insertion loss, in which the waveguide cross is filled with impedance matched metamaterial that effectively suppresses the diffraction of the guided mode in the crossing region, was proposed in [10].

There are only a few works considering the crosstalk noise issue in ONoCs. The crosstalk noise and SNR of a mesh-based ONoC using an optimized crossbar optical router were analyzed in [6]. Moreover, a novel compact high-SNR optical router, called Crux, was proposed to outperform the SNR of large scale ONoCs. Xie *et al.* [11] proposed a formal method to analyze the worst-case crosstalk noise and SNR in arbitrary mesh-based ONoCs. Chan *et al.* [12] proposed a methodology to characterize and model basic photonic blocks, which can form full photonic network architectures, and used a physical-layer simulator to assess the physical-layer and system-level performance of a photonic network. Ding *et al.* [13] proposed a hybrid global router, called GLOW, to provide low power interconnects, while considering the thermal reliability and physical design constraints. Sherwood-droz *et al.* [14] described the fundamental limits for the number of WDM channels and power per channel when using building blocks that include silicon waveguides, silicon microring modulators, and filters. Lin *et al.* [15] developed an analytical model to characterize the crosstalk noise level in a microring-based optical interconnection network.

ONoCs based on the folded-torus topology have been proposed [16]. The novel contribution of this paper is to systematically analyze and model the worst-case crosstalk noise and SNR in folded-torus-based ONoCs using an arbitrary 5×5 optical router. Moreover, we present a novel crosstalk noise and loss analysis platform, called CLAP, which is capable of analyzing crosstalk noise power, power loss, and SNR of ONoCs using an arbitrary optical router. The proposed analyses are based on a hierarchical approach, which starts from the basic optical elements, continues at the optical router level, and ends at the network level. In this way, the proposed formal analytical models at the network level can easily be translated into the device level models for validation. The analytical models for the worst-case crosstalk noise and SNR in folded-torus-based ONoCs are presented. A general 5×5 optical router model, which can be applied to any 5×5 optical router, is considered in our analyses. We analyze different optical links that are among the longest in folded-torus-based ONoCs to find the worst-case SNR link. Case studies of optimized crossbar and Crux optical routers using recent photonic device parameters are presented in this paper. Furthermore, we utilize CLAP to compare the worst-case crosstalk noise and SNR in folded-torus-based and mesh-based ONoCs using optimized crossbar and Crux optical routers. The analyzed folded-torus ONoC is a hybrid structure, consisting of a packet-switched electronic network overlapped by a circuit-switched photonic network, both based on the folded-torus topology. The electronic network is responsible for controlling the photonic network and routing control packets, while the payload data are being exchanged in the photonic network. We assume the use of an on-chip vertical cavity surface emitting laser as the laser source. The proposed systematic formal model does not consider dynamic variations of optical devices such as laser noise and thermal noise.

The rest of this paper is organized as follows. Section II presents the analyses for the basic optical elements and optical routers. The network level analysis and the quantitative simulation results are presented in Section III. Using our new analyzer, CLAP, the proposed analytical models are applied to case studies of folded-torus-based ONoCs using optimized crossbar and Crux optical routers in Section IV. In the same section, we present the worst-case crosstalk noise and SNR comparison in folded-torus-based and mesh-based ONoCs. Finally, the conclusions are drawn in Section V.

II. Basic Optical Elements and Optical Router Analyses

Basic optical elements are the key components in building optical routers for ONoCs. The basic function of optical routers is to direct the optical signal from the source processor toward the destination one. The physical limitations imposed by integration necessitate a compact and low loss design for optical routers. However, without low crosstalk optical routers, the designed ONoC would fail to faultlessly transmit information. In this section, we model and analyze the power loss and crosstalk noise at the device and router levels. The router level analysis is based on a general 5×5 optical router model. Moreover, an abstract model, called router region, is proposed to facilitate the analysis at the network level.

A. Basic Optical Switching Elements

In most of the waveguide crossings used in ONoCs, the latitudinal and longitudinal waveguides are in the same plane.

TABLE I
NOTATIONS FOR LOSSES, CROSSTALK, AND REFLECTANCE COEFFICIENTS

Parameter	Notation
Crossing loss	L_c
Propagation loss	L_p
Power loss per CSE in the OFF state	L_{c0}
Power loss per CSE in the ON state	L_{c1}
Bending loss	L_b
Power loss per PSE in the OFF state	L_{p0}
Power loss per PSE in the ON state	L_{p1}
Crossing's crosstalk coefficient	K_c
Crosstalk coefficient per PSE in the OFF state	K_{p0}
Crosstalk coefficient per PSE in the ON state	K_{p1}
Optical terminator's reflectance coefficient	K_t
Crossing's back-reflection coefficient	K_r

Perfect crossing is not possible because of the coupling of the four branches, or ports, of the intersection in terms of a resonant cavity at the center. Therefore, optical modes propagate with insertion loss from the input port to the output port on the opposite side of the crossing intersection, with some reflection back on the input port and also transmission (crosstalk) to the other outputs. Waveguides and microresonators are the two fundamental optical elements employed to construct basic optical switching elements (BOSEs) and optical routers. Optical routers consist of BOSEs, waveguide crossings, waveguides, and optical terminators. Two types of basic 1×2 optical switching elements are the parallel switching element (PSE) and the crossing switching element (CSE). The PSE includes a microresonator located between two parallel waveguides, as shown in Fig. 1(c). The CSE, depicted in Fig. 2, is a structure consisting of a microresonator adjacently positioned next to a waveguide crossing intersection. BOSEs can be powered on (the ON state) or off (the OFF state) by changing the voltage applied to the microresonator. An optical signal with a wavelength different from the resonant frequency of the microresonator will pass the ring (OFF state) toward the through port. By contrast, when the switch is turned on, the optical signal will couple into the ring and be directed to the drop port (ON state). However, when an optical signal enters the input port of a BOSE, it suffers from insertion loss and crosstalk noise will be generated on the other ports. The crosstalk noise and back-reflection are illustrated as dashed-orange lines in Figs. 1 and 2. In this paper, we consider incoherent crosstalk, whose phase is uncorrelated with the optical signal.

The waveguide crossing, as shown in Fig. 1(a), consists of an input port and three output ports—out1, out2, and out3. We model the insertion loss, crosstalk noise, and back-reflection power in the waveguide crossing, as defined in (1). Table I lists the notations used in the equations in this paper. P_{in} refers to the input power. P_{O1}, P_{O2}, and P_{O3} are the output powers at out1, out2, and out3 ports, respectively. P_{Rc} shows the reflected power on the input port. The basic function of optical terminators, Fig. 1(b), is to avoid the light reflecting back on the transmission line. The reflected power, P_{Rt}, of the optical terminator can be written as (2)

$$P_{O1} = L_c P_{in} \tag{1a}$$
$$P_{O2} = P_{O3} = K_c P_{in} \tag{1b}$$
$$P_{Rc} = K_r P_{in} \tag{1c}$$
$$P_{Rt} = K_t P_{in}. \tag{2}$$

The parallel switching element can be in either the OFF or the ON state [Fig. 1(c)]. The output powers at the through and drop ports as a function of the input optical power can be calculated based on (3) for the OFF state and on (4) for the ON state. In these equations, P_T is the output power at the through port, while P_D shows the output power at the drop port

$$P_{T\,pse,off} = L_{p0} P_{in} \tag{3a}$$
$$P_{D\,pse,off} = K_{p0} P_{in} \tag{3b}$$
$$P_{T\,pse,on} = K_{p1} P_{in} \tag{4a}$$
$$P_{D\,pse,on} = L_{p1} P_{in}. \tag{4b}$$

Utilizing the analytical models of the PSE and the waveguide crossing, the output powers at the add, through, and drop ports of the CSE are derived based on (1), (3), and (4), respectively. Considering Fig. 2, when the CSE is in the OFF state, the output powers at different ports can be calculated based on (5) and when it is in the ON state, (6) calculates the output powers. In these equations, P_T, P_D, and P_A show the output powers at the through, drop, and add ports, respectively. According to Fig. 2(a), the power loss of the CSE in the OFF state, L_{c0}, can be calculated based on the models of the waveguide crossing and the PSE in the OFF state as $L_c L_{p0}$, in which L_{p0} corresponds to the passing loss caused by the MR and L_c is the crossing loss of the waveguide crossing. Similarly, different sources of the power loss and crosstalk noise shown in (5) and (6) can be described. When the CSE is in the ON state, the power loss, L_{c1}, can be calculated by considering the models of the PSE in the ON state and the waveguide crossing, which results in $L_{p1}(1+K_{p1}^2K_c^2)+K_{p1}^2K_c$. Based on this equation, since the crosstalk coefficients are very small numbers ($K_iK_j \cong 0$), L_{c1} can be approximated by L_{p1}

$$P_{T\,cse,off} = L_{c0} P_{in} \tag{5a}$$
$$P_{D\,cse,off} = (K_{p0} + L_{p0}^2 K_c) P_{in} \tag{5b}$$
$$P_{A\,cse,off} = K_c L_{p0} P_{in} \tag{5c}$$
$$P_{R\,cse,off} = K_r L_{p0}^2 P_{in} \tag{5d}$$
$$P_{T\,cse,on} = K_{p1}(L_c(1 + K_c L_{p1}) + K_r L_{p1} K_c) P_{in} \tag{6a}$$
$$P_{D\,cse,on} = L_{c1} P_{in} \tag{6b}$$
$$P_{A\,cse,on} = K_{p1}(K_c(1 + K_c L_{p1}) + K_r L_{p1} L_c) P_{in} \tag{6c}$$
$$P_{R\,cse,on} = K_{p1}^2 K_r P_{in}. \tag{6d}$$

B. General Optical Router Model

The general optical router model, depicted in Fig. 3, is proposed to analyze the crosstalk noise and SNR at the router level, as well as the network level. It is based on a 5×5 optical router and follows the dimension-ordered routing algorithm.

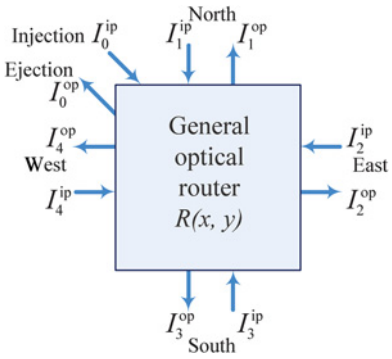

Fig. 3. General 5×5 optical router model.

Considering the general optical router model, the proposed formal method can easily be applied to folded-torus-based ONoCs using an arbitrary 5×5 optical router. In other words, the general router model represents any 5×5 optical router with any physical layout. It has five input and five output ports, including Injection/Ejection, North, East, South, and West. Each port is defined as $I_i^{ip/op}$, in which the subscript i defines the port number and, for different ports, varies from 0 to 4 according to *i=0* for Injection/Ejection, *i=1* for North, *i=2* for East, *i=3* for South, and *i=4* for West. Moreover, the superscript *ip* shows that the port is an input port, and *op* indicates that the port is an output port. The general physical layout, as well as the internal structure of the general optical router model, can be determined when employing a specific optical router.

$L_{i,j}(x, y)$, defined in (7a), is the insertion loss from the ith port to the jth port in the router $R(x, y)$. It includes the switching loss, $S_{Li,j}(x, y)$, caused by the switching elements, CSEs and PSEs, and waveguide crossings inside the optical router $R(x, y)$ as well as the propagation loss inside the optical router, which is calculated by considering the waveguide length between the ith input port and the jth output port, $W_{li,j}(x, y)$, and the propagation loss, L_p. We integrate the propagation loss at the network level into our general optical router model; when the output port is not Ejection, $j \neq 0$, we consider the propagation loss of the waveguide that connects the optical router $R(x, y)$ to the next optical router as described in (7a). D is the hop-length and can be calculated based on (7b) for homogeneous symmetrical ONoCs. S is the chip size (cm^2), and $M \times N$ is the network size

$$L_{i,j}(x, y) = \begin{cases} S_{Li,0}(x, y) L_p^{W_{li,0}(x,y)} & \text{j=0} \\ S_{Li,j}(x, y) L_p^{W_{li,j}(x,y)+D} & \text{j} \neq 0 \end{cases} \tag{7a}$$

$$D \cong \sqrt{\frac{S}{M \times N}} \tag{7b}$$
$$i, j \in \{0, \cdots, 4\}, x \in \{1, \cdots, M\}, y \in \{1, \cdots, N\}.$$

$s_{i,j}(x, y)$ is the status of the optical router $R(x, y)$, while an optical signal is traveling from the ith port to the jth port. The router status is defined in (8). In this equation, I_a^{ip}, I_b^{ip}, I_c^{ip}, I_d^{ip}, and I_e^{ip} are the input ports associated with the output ports I_0^{op}, I_1^{op}, I_2^{op}, I_3^{op}, and I_4^{op}, respectively. -1 is used when the output port is free. For example, $s_{0,2}(x, y)(I_{-1}^{ip}, I_3^{ip}, I_0^{ip}, I_{-1}^{ip}, I_{-1}^{ip})$ indicates that the considered optical signal is traveling from the injection port toward the east port, *i=0*, *j=2*, and *c=0*, while there is another optical signal traveling from the south port to the north port, *b=3*, which mixes with the considered optical signal and introduces crosstalk noise to it in the router $R(x, y)$. Furthermore, it shows that no signal exists at the ejection, south output, and west output ports, $a = d = e = -1$

$$\begin{aligned} &s_{i,j}(x, y) = (I_a^{ip}, I_b^{ip}, I_c^{ip}, I_d^{ip}, I_e^{ip}) \\ &a \in \{-1, 1, 2, 3, 4\} \\ &b \in \{-1, 0, 2, 3, 4\} \\ &c \in \{-1, 0, 4\} \\ &d \in \{-1, 0, 1, 2, 4\} \\ &e \in \{-1, 0, 2\}. \end{aligned} \tag{8}$$

$P_{i,j}(x, y)$, calculated in (9), is defined as the optical power output by the jth port caused by the optical power, $P_i^{in}(x, y)$, injected into the ith port in the optical router $R(x, y)$

$$P_{i,j}(x, y) = P_i^{in}(x, y) L_{i,j}(x, y) \tag{9}$$
$$i, j \in \{0, \cdots 4\}, x \in \{1, \cdots, M\}, y \in \{1, \cdots, N\}.$$

$N_{i,j}(x, y, s_{i,j}(x, y))$, as shown in (10), is defined as the crosstalk noise added to the optical signal traveling from the ith port to the jth port, and $K_{i,j,m}(s_{i,j}(x, y))$ is defined as the coefficient for the crosstalk noise introduced by $P_m^{in}(x, y)$ onto the same optical signal in the router $R(x, y)$ under status s

$$N_{i,j}(x, y, s_{i,j}(x, y)) = \sum_{m=0}^{4} \left(P_m^{in}(x, y) K_{i,j,m}(s_{i,j}(x, y)) \right)$$
$$i, j \in \{0, \ldots, 4\}, x \in \{1, \ldots, M\}, y \in \{1, \ldots, N\}. \tag{10}$$

SNR is defined as the ratio of the signal power to the power of the crosstalk noise corrupting the signal and can be written as (11), in which P_S is the optical signal power and P_N is the crosstalk noise power

$$SNR = 10 \log \left(\frac{P_S}{P_N} \right). \tag{11}$$

C. Router Region Model

An abstract router region model is presented to resemble folded-torus-based ONoCs with mesh-based ONoCs, as well as to compact SNR analytical equations at the network level. Fig. 4 shows the router region for the folded-torus-based ONoCs. As the figure shows, it consists of nine input and nine output ports. The input (output) ports of the general optical router, located inside the router region, can connect to any of the input (output) ports of the router region. Using the abstract router region, the waveguide crossings and bendings at the network level are integrated into the router level model. Therefore, in each router region, there are a number of input ports that do not go through the optical router. There are a total of 16 different router regions in folded-torus-based ONoCs when M and N are even numbers. Another seven router regions can be introduced when the network size is an odd number. Fig. 5 indicates 23 different router regions defined in folded-torus-based ONoCs. Each router region consists of a general

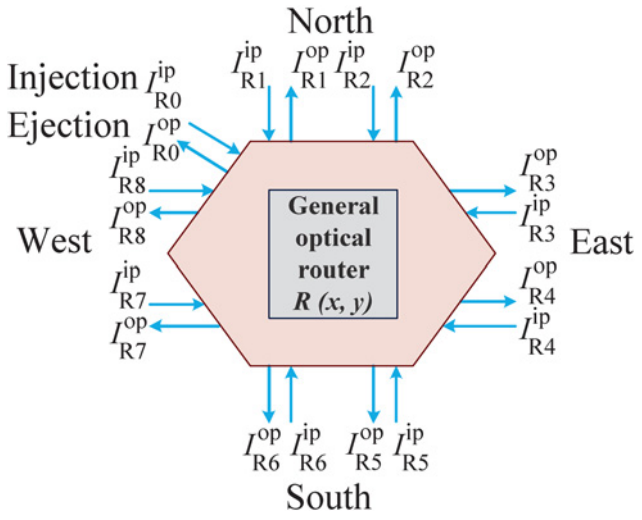

Fig. 4. Abstract router region model defined for folded-torus-based ONoCs.

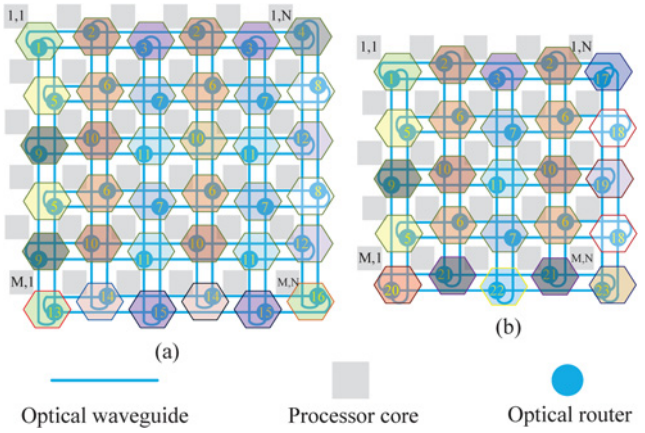

Fig. 5. Router regions defined in the folded-torus-based ONoCs when M and N are (a) even numbers and (b) odd numbers.

optical router, a number of waveguide crossings and, in some cases, waveguide bendings.

The router region model can be defined similarly to the general optical router model. $I_{Ri}^{ip/op}$ is the ith port, while i indicates the port number, as depicted in Fig. 4. The superscript *ip/op* tells whether the port is an input port, where *ip* is used, or is an output one, where *op* is used. $L^R_{i,j}(x, y)$ is defined as the insertion loss from the ith port to the jth port in the router region $R^2(x, y)$, as shown in (12). As an example, the insertion losses in the router region 1, $R^2(1, 1)$, as shown in Fig. 5, are calculated in Appendix A. The general router model status determines the status of the router region

$$L^R_{i,j}(x, y) = \begin{cases} L_{i,j}(x, y)L_c^k L_b^l & \text{enters optical router} \\ L_c^k L_b^l & \text{otherwise} \end{cases}$$
$$i, j \in \{0, \cdots, 8\}, k \in \{0, 2, 4, \cdots\}, l \in \{0, 1, 2, \cdots\}. \tag{12}$$

$P^R_{i,j}(x, y)$ is defined as the optical power output by the jth port caused by the optical power injected into the ith port in the router region $R^2(x, y)$. This power can be calculated based on (13), in which $P^{in}_{Ri}(x, y)$ is the optical power injected into the ith input port of the router region $R^2(x, y)$

$$P^R_{i,j}(x, y) = P^{in}_{Ri}(x, y)L^R_{i,j}(x, y)$$
$$i, j \in \{0, \cdots, 8\}, x \in \{1, \cdots, M\}, y \in \{1, \cdots, N\}. \tag{13}$$

$N^R_{i,j}(x, y)$, calculated in (14), is defined as the crosstalk noise added to the optical signal traveling from the ith port to the jth port in the router region $R^2(x, y)$. $K^R_{i,j,m}(s_{i,j}(x, y))$ is defined as the crosstalk coefficient introduced by $P^{in}_{Rm}(x, y)$ onto the optical signal traveling from the ith port to the jth port in the router region $R^2(x, y)$ under status s

$$N^R_{i,j}(x, y, s_{i,j}(x, y)) = \sum_{m=0}^{8} \left(P^{in}_{Rm}(x, y)K^R_{i,j,m}(s_{i,j}(x, y))\right)$$
$$i, j \in \{0, \cdots, 8\}, x \in \{1, \cdots, M\}, y \in \{1, \cdots, N\}. \tag{14}$$

III. Crosstalk Noise in Folded-Torus-Based ONoCs

The worst-case crosstalk noise and SNR of the folded-torus-based ONoCs are analyzed in this section. The analyses at the network level are based on the proposed device and router level models, and hence can be translated into the initial device level models for validation. The proposed analytical models at the basic device level can be used in any topology, while the optical router level models can be adapted to other topologies as long as a 5×5 optical router is used. However, the systematic worst-case SNR analysis at the network level is dependent on the topology; different topologies have various properties that result in different worst-case SNR analyses. Furthermore, to analyze the worst-case SNR, the worst-case statuses of the optical routers, which are not the same in different topologies, need to be considered. Therefore, while the same hierarchical approach should be followed, to analyze the worst-case crosstalk noise and SNR in other topologies, one needs to analytically model the optical router level based on the proposed device level models and then apply those models to study the worst-case SNR at the network level. The dimension-ordered routing algorithm, which is well known as the XY routing algorithm, is used in the network. We suppose that M and N are both even numbers.

An optical signal suffers from power loss when it passes through a router region. The power loss is caused by the waveguide crossings, waveguide bendings, and most importantly, the optical router located inside the region. The power loss of an optical link is proportional to its hop length. The more router regions passed by the optical link, the higher the power loss is. Obviously, the maximum loss link is the longest one, while the minimum loss link has the shortest length. It is necessary to find the worst-case SNR in the network since it determines the feasibility of folded-torus-based ONoCs. The worst-case SNR link is the one that passes through as many as possible of the router regions and, at the same time, has high crosstalk noise introduced by the noise introducing optical links from neighboring routers. Considering the previously mentioned conditions, the maximum loss link may not be the worst-case SNR link; although it suffers from the highest power loss compared with the shorter links,

the crosstalk noise power accumulated on the shorter links can be higher, resulting in worse SNR. We analyze different optical links that are among the longest in the folded-torus-based ONoCs to find the wort-case SNR link candidates in the network.

A. Different Longest Optical Links Analyses

To enable the worst-case crosstalk noise and SNR analyses in the folded-torus-based ONoCs, some assumptions are made. First, the power loss for the same input and output pair, but different optical routers, is the same. Therefore, $L_{i,j}(x_0, y_0)$ can be simplified as $L_{i,j}$, which is the insertion loss of an optical signal traveling from the ith input port to the jth output port independent of the optical router location. This assumption is shown is (15). The same assumption is valid for the same router regions but in different locations in the network. Second, we suppose that the signal power at the injection port of different optical router regions is the same. Finally, (16) explains the last assumption. Moreover, the proposed analyses consider the first-order crosstalk noise, as shown in (17)

$$L_{i,j}(x_0, y_0) = L_{i,j}(x_1, y_1) = L_{i,j} \tag{15}$$

$$L_{0,j_0} \geq L_{0,j_1} L_{(j_1+1) mod 4+1, j_0} \quad j_0, j_1 \in \{1, \cdots, 4\} \tag{16}$$

$$K_{i_0,j_0,m_0} K_{i_1,j_1,m_1} \approx 0 \quad i_0, j_0, m_0, i_1, j_1, m_1 \in \{0, \cdots, 8\}. \tag{17}$$

The insertion loss of different optical links that are among the longest and the crosstalk noise added to these links needs to be calculated. We start with the very longest optical link. Fig. 6 indicates four of the longest optical links in the folded-torus-based ONoCs, which have the worst-case SNR received at their destinations. The insertion loss of the longest link [Fig. 6(a)] is calculated in (18). In this equation, $PL^R_{(x_0,y_0),(x_1,y_1)}$ represents the signal power for the optical signal traveling from the processor core (x_0, y_0) toward the core (x_1, y_1). The six terms on the right-hand side of the equation represent, respectively, the input power, the insertion loss from the source processor to the first router region, insertion losses on the X-section of the link, the insertion loss at the router region where the link turns from the X to Y-section, insertion losses on the Y-section of the link, and the insertion loss at the router region connected to the destination processor. The first superscript R stands for the router region and the second one is the exponent

$$PL^R_{(1,1),(M,N)} = P_{in} L^R_{0,4} L^{R,N-2}_{7,4} L^R_{7,6} L^{R,M-2}_{1,6} L^R_{1,0}. \tag{18}$$

In Fig. 6, the dotted green lines show the crosstalk noise added to the optical signal at the router level, while the dashed orange lines illustrate the crosstalk noise added at the network level. Considering all of the possible traffic patterns, these noise introduction links are determined in such a way as to guarantee the worst-case crosstalk noise power received at the destination of an optical signal. For example, in Fig. 6(a) for the router region $R^2(1, 1)$, the optical signal traveling from the injection port to the east port is mixed with the optical signals from neighboring router regions into the east and south ports. Using (14), the power of this crosstalk noise is $N^R_{0,4}(1, 1) = P^{in}_{R3}(1, 2)K^R_{0,4,3} + P^{in}_{R4}(1, 3)K^R_{0,4,4} + P^{in}_{R5}(2, 1)K^R_{0,4,5} + P^{in}_{R6}(3.1)K^R_{0,4,6}$. In this equation, for example, $P^{in}_{R3}(1, 2) = P_{in} L_{0,4} L_b$ is the optical power injected into the router region $R^2(1, 2)$; it goes to the eighth port of the same router region, then enters the third port of the router region $R^2(1, 1)$, and finally mixes with the considered optical signal at this router region. The crosstalk noise added to the optical signals in the other router regions can be calculated in the same way. Also, this approach can be used to translate the crosstalk noise and crosstalk noise power equations in Appendix B into the initial device level models. The SNR of the longest optical link, indicated in Fig. 6(a), can be calculated as shown in (19). In this equation, P_{N1} is the crosstalk noise power at the destination of the longest optical link. The detailed analytical equations for crosstalk noise power and SNR equations for the optical links that are among the longest are described in Appendix B

$$SNR_{(1,1),(M,N)} = 10 \log \left(\frac{PL^R_{(1,1),(M,N)}}{P_{N1}} \right). \tag{19}$$

The second, third, fourth, and fifth longest optical links are illustrated in Figs. 7–10, respectively. We pick four of each longest optical link which have the worst-case SNR at their destinations compared with the other links of the same length and analyze the power loss of each of these optical links. The signal power at the destination of the second, third, fourth, and

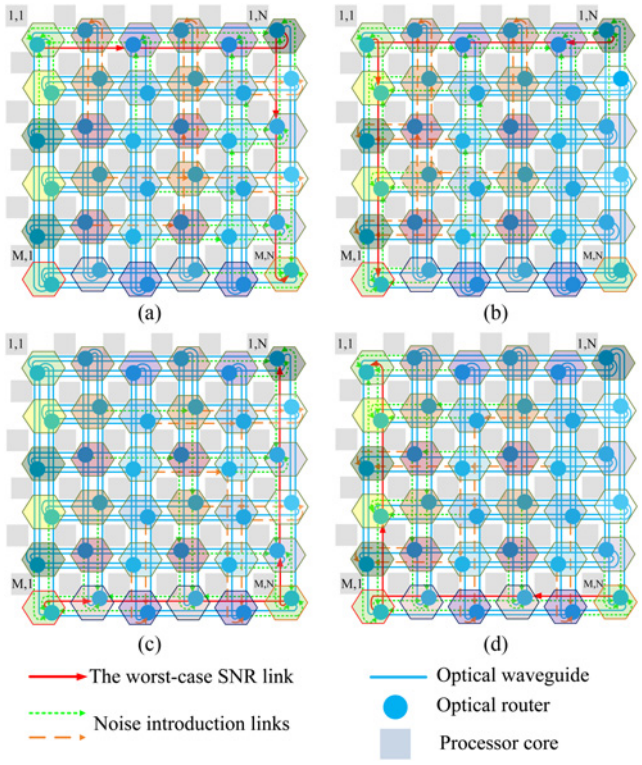

Fig. 6. Longest optical link in an M×N folded-torus-based ONoC. (a) (1, 1) to (M, N). (b) (1, N) to (M, 1). (c) (M, 1) to (1, N). (d) (M, N) to (1, 1).

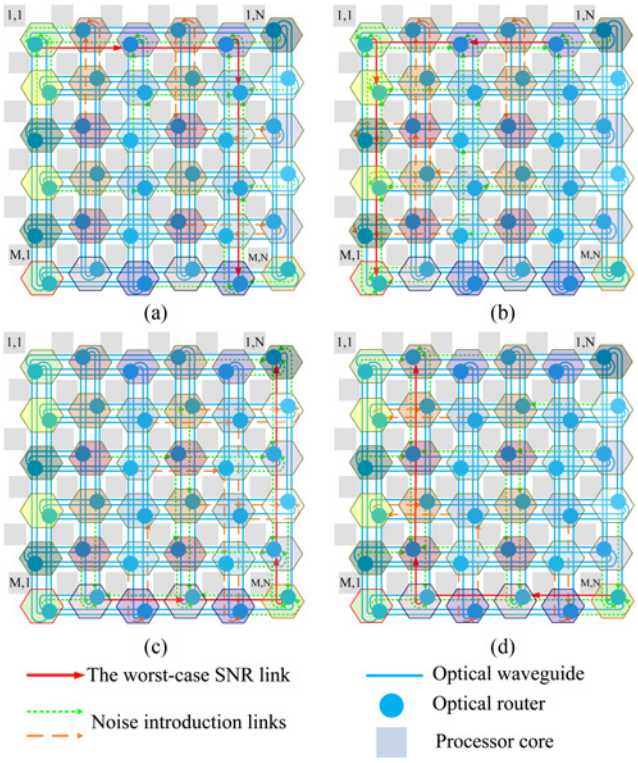

Fig. 7. Second longest optical link in an M×N folded-torus-based ONoC. (a) (1, 1) to (M, N-1). (b) (1, N-1) to (M, 1). (c) (M, 2) to (1, N). (d) (M, N) to (1, 2).

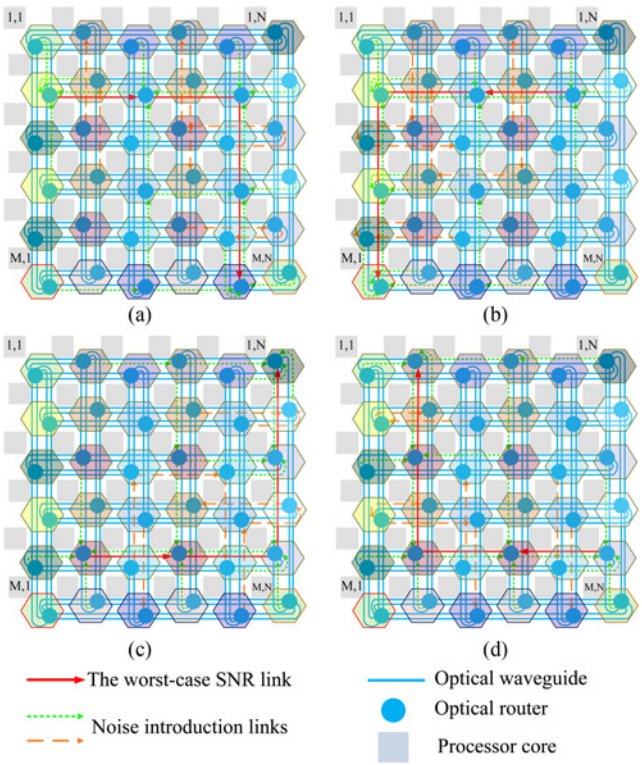

Fig. 8. Third longest optical link in an M×N folded-torus-based ONoC. (a) (2, 1) to (M, N-1). (b) (2, N-1) to (M, 1). (c) (M-1, 2) to (1, N). (d) (M-1, N) to (1, 2).

fifth longest links is calculated in (20), (21), (22), and (23), respectively

$$PL^{R}_{(1,1),(M,N-1)} = P_{in} L^{R}_{0,4} L^{R,N-3}_{7,4} L^{R}_{7,5} L^{R,M-2}_{2,5} L^{R}_{2,0} \tag{20}$$

$$PL^{R}_{(2,1),(M,N-1)} = P_{in} L^{R}_{0,4} L^{R,N-3}_{7,4} L^{R}_{7,5} L^{R,M-3}_{2,5} L^{R}_{2,0} \tag{21}$$

$$PL^{R}_{(2,3),(M,N-1)} = P_{in} L^{R}_{0,4} L^{R,N-5}_{7,4} L^{R}_{7,5} L^{R,M-3}_{2,5} L^{R}_{2,0} \tag{22}$$

$$PL^{R}_{(2,5),(M,N-1)} = P_{in} L^{R}_{0,4} L^{R,N-7}_{7,4} L^{R}_{7,5} L^{R,M-3}_{2,5} L^{R}_{2,0}. \tag{23}$$

The crosstalk noise added to these optical links can be calculated following the same principles described for the longest optical link. The SNR of these longest optical links is calculated in (24), (25), (26), and (27). In these equations, P_{Nl} is the crosstalk noise power received at the destination of the lth longest optical link

$$SNR_{(1,1),(M,N-1)} = 10 \log \left(\frac{PL^{R}_{(1,1),(M,N-1)}}{P_{N2}} \right) \tag{24}$$

$$SNR_{(2,1),(M,N-1)} = 10 \log \left(\frac{PL^{R}_{(2,1),(M,N-1)}}{P_{N3}} \right) \tag{25}$$

$$SNR_{(2,3),(M,N-1)} = 10 \log \left(\frac{PL^{R}_{(2,3),(M,N-1)}}{P_{N4}} \right) \tag{26}$$

$$SNR_{(2,5),(M,N-1)} = 10 \log \left(\frac{PL^{R}_{(2,5),(M,N-1)}}{P_{N5}} \right). \tag{27}$$

B. Worst-Case SNR Link Candidates in Folded-Torus-Based ONoCs

The SNR of the first five longest optical links in the folded-torus-based ONoCs is analyzed. In this subsection, an effort is made to find the worst-case SNR link candidates among these five longest links.

Considering the SNR equation for the fourth longest optical link, the equation can be rewritten as (28) by grouping the numerator and the denominator into different parameters [see (36) and (38) in Appendix B]. Applying (28) to the SNR equation of the fifth longest link results in the conclusion made in (29), in which the right-hand side shows the SNR of the fifth longest link

$$SNR_{(2,3),(M,N-1)} = 10log \left(\frac{a}{b_1 + b_2 + b_3} \right). \tag{28}$$

According to (29) and considering the fact that $Q > 1$ and $C > 0$, it is proved that the SNR of the fourth longest optical link is smaller than the SNR of the fifth longest

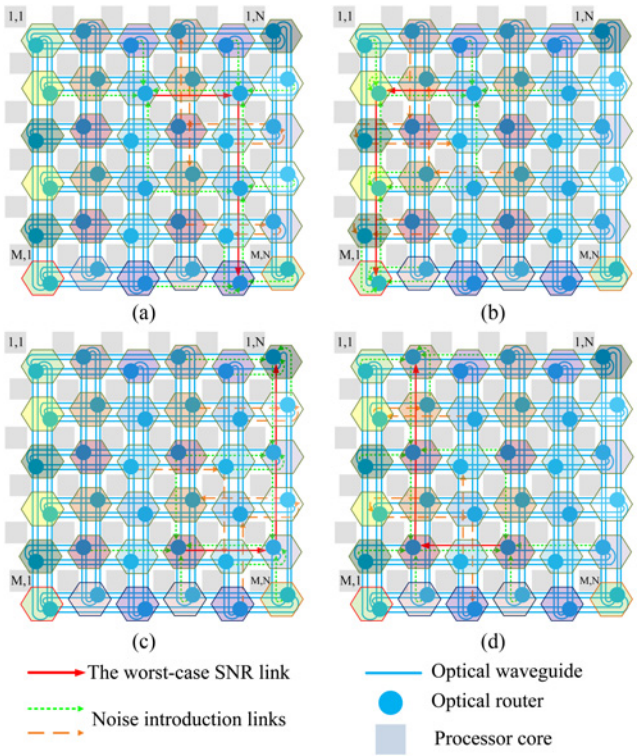

Fig. 9. Fourth longest optical link in an M×N folded-torus-based ONoC. (a) (2, 3) to (M, N-1). (b) (2, N-3) to (M, 1). (c) (M-1, 4) to (1, N). (d) (M-1, N-2) to (1, 2).

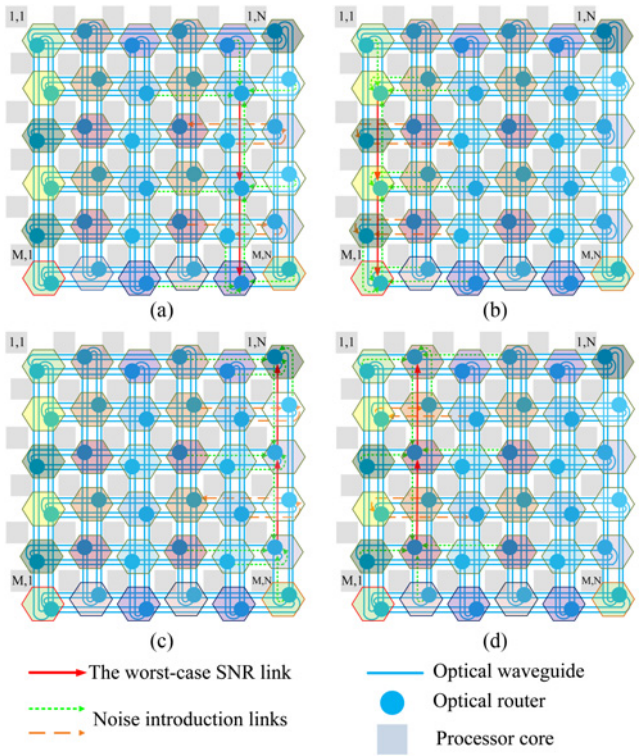

Fig. 10. Fifth longest optical link in an M×N folded-torus-based ONoC. (a) (2, 5) to (M, N-1). (b) (2, N-5) to (M, 1). (c) (M-1, 6) to (1, N). (d) (M-1, N-4) to (1, 2).

one. The worst-case crosstalk noise added to the optical links shorter than the fourth longest optical link follows the same mathematical pattern. In other words, the SNR comparison among the optical links shorter than the fourth one only depends on the link's power loss; the shorter the optical link, the higher the SNR is. On the other hand, there is no explicit mathematical relationship among the SNR equations of the first four longest optical links due to the diversity of the worst-case crosstalk noise mathematical patterns for these links. Therefore, the worst-case SNR link candidates in the folded-torus-based ONoCs must be the first, second, third, and fourth longest optical links in the network. Applying a specific optical router results in only one worst-case SNR link, which is among the nominated optical links. The same conclusion is valid when M and N are odd numbers

$$\frac{a}{b_1+b_2+b_3} < \frac{Qa}{Qb_1+b_2+b_3-C} \tag{29}$$

where

$$Q = L_{4,2}^{-1}L_c^{-6}$$

$$C = L_{4,3}L_{1,3}^{\frac{M}{2}-2}L_{1,0}(L_c^{3M-4}L_{4,2}^{\lfloor\frac{N-6}{2}\rfloor}L_c^{\lfloor\frac{N-6}{2}\rfloor}N_c(2,4) + L_c^{3M}L_{4,2}^{\lfloor\frac{N-7}{2}\rfloor}L_c^{\lfloor\frac{N-7}{2}\rfloor}N_{4,2}(2,5)).$$

C. Quantitative Simulation

The quantitative simulation of the worst-case SNR link candidates is performed using MATLAB. Referring to the notations in Table I, we employ a waveguide crossing with a size of 450 nm × 200 nm and with $L_c = -0.04$ dB, $K_c = -40$ dB, and $K_r \cong 0$ [10]. Moreover, L_{p0}, L_{p1}, K_{p0}, and K_{p1} are -0.005 dB, -0.5 dB, -20 dB, and -25 dB, respectively [12]. L_b is equal to $-0.005\,\text{dB}/90^\circ$ and K_t is equal to -50 dB [17], [18]. Also, L_p = -0.247 dB/cm [20]. The diameter of the microresonator is 10 μm. It is assumed that the injection power, P_{in}, in different optical routers is the same and is equal to 0 dBm. The same parameters are used for our case study in the next section. The proposed analytical models are based on the notations described in Table I and the above parameters are used only as an example.

First, the router region model is expanded to the optical router model in the SNR equations. Moreover, to simplify the expanded equations, we suppose that all of the insertion losses are equal; $L_{i,j} = L$, in which L is the average insertion loss in the general optical router model. Also, it is assumed that $K_{i,j,m} = K$, where K is the arithmetic mean of the crosstalk noise coefficients, K_c, K_{p0}, and K_{p1}. The resulting equations are, in the general form, shown in (30). Using the expanded simplified SNR equations, we perform the quantitative simulation for the longest link as an example. Fig. 11(a) indicates the SNR of the longest optical link under average loss values of -0.1 dB and -0.4 dB. The z-axis is reversed to perfectly show the results. As can be seen, the SNR reduces as the average loss increases and the network scales. Moreover, one can see that when $M = N$, the SNR is the best. This fact is shown in Fig. 11(b), in which when $M \times N = C$ and C is a constant number, M equals N results in the best SNR. In

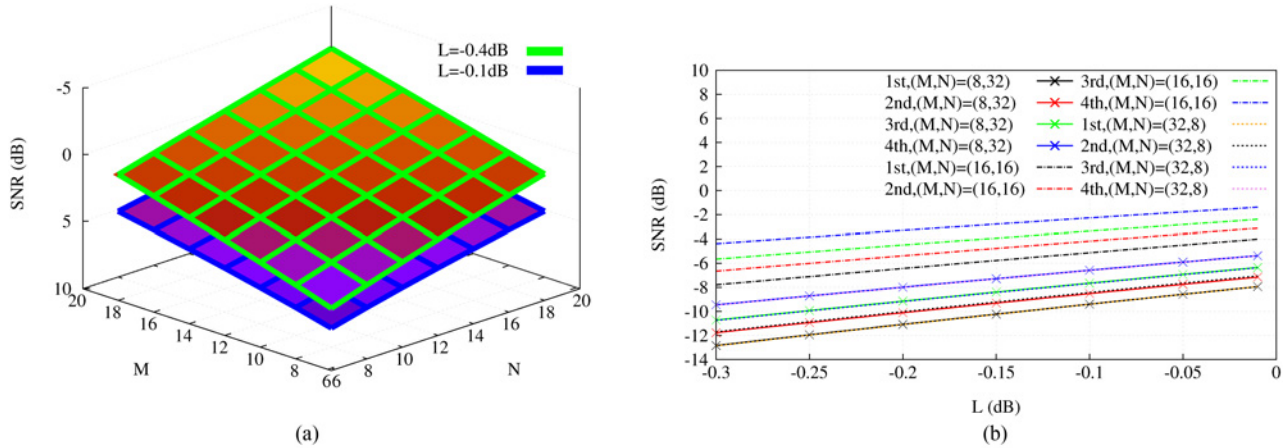

Fig. 11. SNR of the first, second, third, and fourth longest optical links in an M×N folded-torus-based ONoC. (a) Longest link. (b) M×N=256.

other words, symmetric folded-torus-based ONoCs have the best SNR. Furthermore, closer values of M and N result in higher SNR. In the same figure, the SNR is almost the same for $M \times N = C$ and $N \times M = C$, which shows the symmetry feature of the folded-torus ONoCs. Quantitative simulations of the other candidates can be similarly performed

$$SNR_{(x_0,y_0),(x_1,y_1)}(L, M, N) = 10log\left(\frac{P_S(L, M, N)}{P_N(L, M, N)}\right). \quad (30)$$

In order to find the scalability constraints in folded-torus-based ONoCs, Fig. 12 indicates the relationship between the average loss in the general optical router, L, and the network size when the signal power and the noise power are the same (SNR = 0 dB) and when $M = N$, which results in the best SNR. The loss decreases dramatically with the increase in the network size. Given the network size and its related average loss value in this figure, the noise power exceeds the signal power for higher loss values. Moreover, as shown in this figure, for network sizes smaller than 6×6, the signal power is higher than the noise power all the time. However, when the network size is larger than 12×12, the noise power is always higher than the signal power, which shows the critical behavior of crosstalk noise in the folded-torus-based ONoCs. Table II indicates the related signal power and crosstalk noise power values for different network sizes in Fig. 12 when the input power equals 0 dBm. Some of the cells in this table are empty since the signal power and crosstalk noise power cannot be equal within the average loss value used in Fig. 12. For example, when the network size is 6×6, the average loss value needs to be higher than −3 dB to make the received signal power and crosstalk noise power equal at the destination of the third and the fourth longest optical links.

IV. Case Study

Using our proposed analytical models, we present case studies of folded-torus-based ONoCs using the optimized crossbar and Crux optical routers. Moreover, the worst-case crosstalk noise and SNR of folded-torus-based and mesh-based ONoCs using these optical routers are compared, utilizing our novel crosstalk noise and loss analysis platform, CLAP.

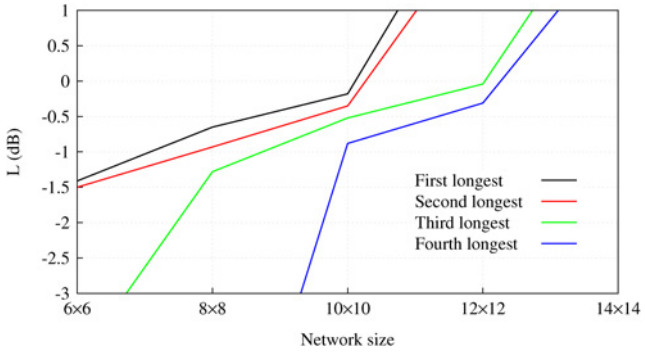

Fig. 12. Relationship between the average loss in the general optical router model and the network size when the signal power is equal to the noise power in the folded-torus-based ONoCs.

A. Crosstalk Noise and Loss Analysis Platform (CLAP)

Fig. 13 illustrates the internal structure of CLAP. The publicly released CLAP is implemented in C++, and it is available online with documentation at [19]. CLAP analyzes the crosstalk noise power, power loss, and SNR in ONoCs of any network size at the system level. As can be seen from the figure, CLAP's internal structure includes inputs, a CLAP analyzer, outputs, a device library, and a network library. CLAP has a complete library of photonic devices and BOSEs to construct arbitrary optical routers and ONoCs, including I/Os, waveguide crossings, waveguide bendings, waveguides, optical terminators, microresonators, parallel switching elements, and crossing switching elements. Folded-torus-based and mesh-based ONoCs are considered the two network architectures in the network library. CLAP can easily be extended to include more ONoC architectures. We consider three input files in CLAP, including device parameters, router structure, and network configuration. The power loss values, crosstalk coefficients, reflectance coefficients, waveguide dimensions, the microresonator diameter, and the injection power can be defined in device parameters as inputs. router structure includes the definition of the optical router structure, while network configuration consists of the network size, chip size, and the communication pattern among the processor cores.

TABLE II
RELATED SIGNAL POWER (UPPER ROW IN BLACK) AND CROSSTALK NOISE POWER (LOWER ROW IN RED) VALUES IN FIG. 12 WHEN THE INPUT POWER EQUALS 0 DBM

Network size	1st longest	2nd longest	3rd longest	4th longest
6×6	-15.01dBm	-15.95dBm	-	-
	-15.04dBm	-15.27dBm	-	-
8×8	-12.88dBm	-13.83dBm	-14.69dBm	-
	-13dBm	-13.91dBm	-14.90dBm	-
10×10	-10.94dBm	-11.84dBm	-12.34dBm	-13.75dBm
	-11.17dBm	-12.04dBm	-12.82dBm	-13.84dBm
12×12	-	-	-10.09dBm	-11.76dBm
	-	-	-10.90dBm	-11.96dBm

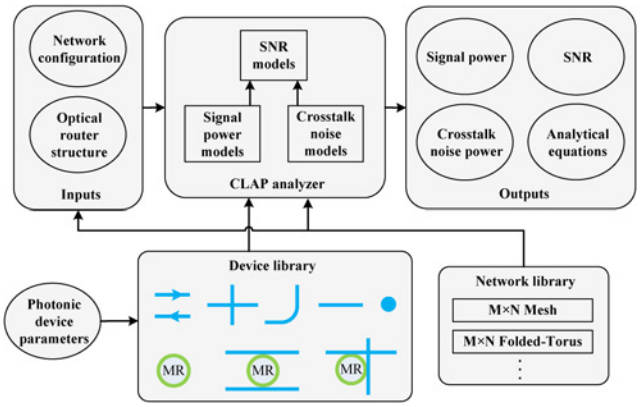

Fig. 13. CLAP's internal structure.

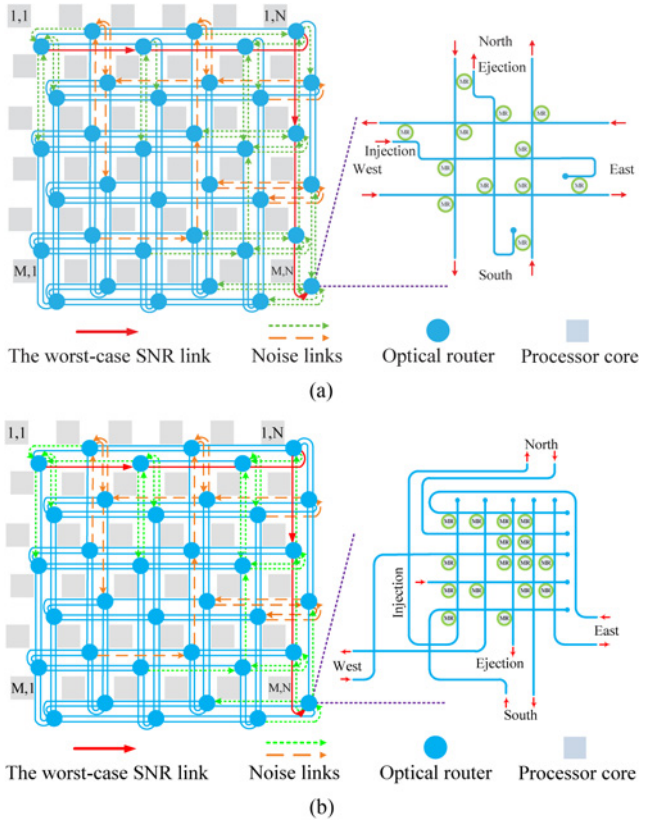

Fig. 14. Worst-case SNR links in folded-torus-based ONoCs using (a) Crux optical router and (b) optimized crossbar optical router.

Based on our proposed analytical models, the signal power, crosstalk noise power, and SNR at the destination of a specific optical signal, defined by the user, can be analyzed in the CLAP analyzer. The analyzer is optimized to speed up the computations for large scale ONoCs. CLAP is capable of analyzing the propagation loss at the device, router, and network levels by using the defined dimensions for the waveguides and microresonators. CLAP also generates the analytical equations used to analyze the signal power and crosstalk noise power in ONoCs.

B. Analyses and Results

The optimized crossbar and Crux optical routers are shown in Fig. 14. Both optical routers have five bidirectional ports, including Injection/Ejection, North, East, South, and West. The SNR of the first four longest links is analyzed and compared to find the worst-case SNR link in the network. Results show that the optical links from the processor core *(1, 1)* toward the processor core *(M, N)*, shown in Fig. 14(a) and (b), have the worst-case SNR in folded-torus-based ONoCs using optimized crossbar and Crux optical routers. As the figures indicate, the communication pattern that leads to the worst-case SNR at the destination of the optical links varies when different optical routers are used. The proposed analytical models are adaptable to folded-torus-based ONoCs using different optical router structures since they are based on the general optical router model. The insertion loss suffered by the worst-case SNR link in folded-torus-based ONoCs using the Crux optical router is calculated in (31). In this equation, the first subscripts denote the router input ports, and the second ones show the router output ports

$$L_{SNR_{min}} = L_{in,e} L_{w,e}^{\frac{N}{2}-1} L_{e,s} L_{n,s}^{\frac{M}{2}-1} L_{s,ej} L_c^{3M+3N-4} L_b^2. \quad (31)$$

The total crosstalk noise power can be calculated by adding the crosstalk noise from each optical router on the link, while the total insertion loss of the link is given by (31). The worst-case SNR in the folded-torus-based ONoCs using the Crux optical router, depicted in Fig. 14(a), is calculated in (32). The detailed analytical equations are described in Appendix B. Following the same approach, the insertion loss and crosstalk noise added to the worst-case SNR link in folded-torus-based ONoCs using the optimized crossbar optical router, shown in Fig. 14(b), can be calculated. The worst-case crosstalk noise and SNR in mesh-based ONoCs using optimized crossbar and Crux optical routers were analyzed in [6]

$$SNR_{min,Crux} = 10 \log \left(\frac{P_{in} L_{SNR_{min}}}{P_{N,Crux}} \right). \quad (32)$$

Using the device parameters defined in Section III-C and CLAP, we compare the worst-case crosstalk noise and SNR in folded-torus-based and mesh-based ONoCs using optimized crossbar and Crux optical routers. Fig. 15 depicts the worst-case SNR comparison between folded-torus-based and mesh-based ONoCs using the optimized crossbar and Crux optical routers under different network sizes. As the figure shows, the SNR decreases when the network scales, and this reduction is at a more rapid rate when the optimized crossbar router is used. For example, as shown in Fig. 15, the

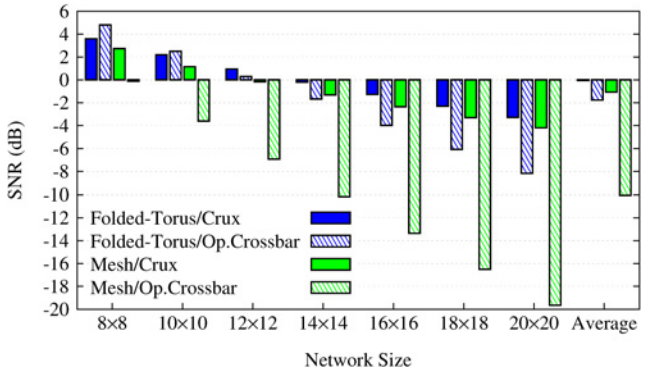

Fig. 15. Worst-case SNR comparison.

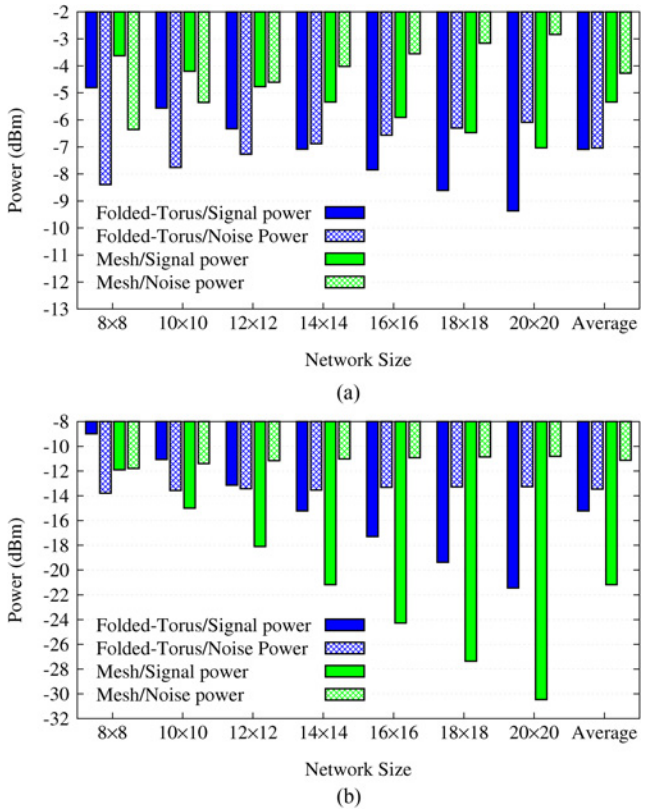

Fig. 16. Worst-case signal power and crosstalk noise power comparison. (a) Using Crux optical router. (b) Using optimized crossbar optical router.

average worst-case SNR in folded-torus-based ONoCs, when the optimized crossbar router is used, equals −2 dB and, when the Crux optical router is used, equals 0.1 dB. Furthermore, the folded-torus has higher worst-case SNR compared with the mesh, and when the Crux optical router is used, both architectures have the highest worst-case SNR.

Fig. 16 compares the worst-case signal power and crosstalk noise power in folded-torus-based and mesh-based ONoCs using the optimized crossbar and Crux optical routers. According to this figure, as the network size increases, the worst-case signal power declines, while the crosstalk noise power increases. Using the optimized crossbar optical router, as shown in Fig. 16(b), it can be seen that the folded-torus has better worst-case signal power and crosstalk noise compared with the mesh, since the hop-length of the worst-case SNR link in folded-torus-based ONoCs is shorter than that in mesh-based ONoCs. However, when the Crux optical router is used, as depicted in Fig. 16(a), the mesh-based ONoCs have higher worst-case signal power compared with folded-torus ONoCs, but the worst-case crosstalk noise power is also considerably higher in the mesh. The folded torus introduces extra waveguide crossing and bending loss at the network level, which diminishes the signal power and the crosstalk noise power. Furthermore, both the signal power and crosstalk noise power are higher compared with ONoCs using the optimized crossbar router. This is due to the fact that the Crux optical router introduces lower power loss compared with the optimized crossbar, which not only results in better signal power, but also higher crosstalk noise power. Another important observation is that for the network sizes larger than 12×12 in folded-torus-based ONoCs using the optimized crossbar and Crux optical routers, larger than 6×6 in mesh-based ONoCs using the optimized crossbar, and larger than 10×10 in mesh-based ONoCs using the Crux optical router, the noise power exceeds the signal power. For example, when the network size is 20×20 and the optimized crossbar optical router is used, the signal power and crosstalk noise power in the folded-torus-based ONoC are −21.4 dBm and −13.3 dBm, respectively, and in the mesh-based ONoC are equal to −30.5 dBm and −10.8 dBm. However, when the Crux optical router is used, the signal power and crosstalk noise power in the folded-torus-based ONoC are −9.4 dBm and −6.1 dBm, respectively, and in the mesh-based ONoC are equal to −7.1 dBm and −2.8 dBm.

V. Conclusion

Crosstalk noise is an intrinsic characteristic of photonic devices widely used in constructing ONoCs. For the first time, we systematically model and analyze the worst-case crosstalk noise and SNR in folded-torus-based ONoCs. Furthermore, a novel crosstalk noise and loss analysis platform called CLAP, which is capable of analyzing crosstalk noise, power loss, and SNR of arbitrary ONoCs, is presented. The analytical crosstalk noise and SNR models are hierarchically proposed at the basic photonic device level, optical router level, and network level. We consider a general 5×5 optical router model that enables worst-case crosstalk noise and SNR analyses in folded-torus-based ONoCs using an arbitrary 5×5 optical router. We prove that the worst-case SNR link in folded-torus-based ONOCs is among the first, second, third, and fourth longest optical links. We also show that when the network size is equal to a constant number, $M \times N = C$ and C is a constant, the best SNR can be achieved only when $M = N$. Utilizing the proposed analytical method, the worst-case crosstalk noise and SNR of folded-torus-based ONoCs using optimized crossbar and Crux optical routers are analyzed as case studies. Moreover, the worst-case crosstalk noise and SNR in folded-torus-based and mesh-based ONoCs are compared. We also find that crosstalk noise considerably restricts the scalability of ONoCs; for example, in the worst-case, when the optimized crossbar router is used, for the network sizes larger than 12×12 in folded-torus-based ONoCs and larger than 6×6 in mesh-based ONoCs, the crosstalk noise power exceeds the signal power.

$$
\begin{array}{lll}
L^R_{0,3}(x,y) = L_{0,4}(x,y)L_b & L^R_{0,4}(x,y) = L_{0,2}(x,y)L_c^2 & L^R_{0,5}(x,y) = L_{0,1}(x,y)L_c^2L_b \\
L^R_{0,6}(x,y) = L_{0,3}(x,y) & L^R_{3,0}(x,y) = L_{4,0}(x,y)L_b & L^R_{3,4}(x,y) = L_{4,2}(x,y)L_c^2L_b \\
L^R_{3,5}(x,y) = L_{4,1}(x,y)L_c^2L_b^2 & L^R_{3,6}(x,y) = L_{4,3}(x,y)L_b & L^R_{4,0}(x,y) = L_{2,0}(x,y)L_c^2 \\
L^R_{4,3}(x,y) = L_{2,4}(x,y)L_c^2L_b & L^R_{4,5}(x,y) = L_{2,1}(x,y)L_c^4L_b & L^R_{4,6}(x,y) = L_{2,3}(x,y)L_c^2 \\
L^R_{5,0}(x,y) = L_{1,0}(x,y)L_c^2L_b & L^R_{5,6}(x,y) = L_{1,3}(x,y)L_c^2L_b & L^R_{6,0}(x,y) = L_{3,0}(x,y) \\
L^R_{6,5}(x,y) = L_{3,1}(x,y)L_c^2L_b &&
\end{array} \tag{33}
$$

$$
N^R_{i,j_{(1st)}}(x,y,ws_{i,j}(x,y)) = \tag{34}
$$

$$
\begin{cases}
P_{in}(L^R_{0,8}K^R_{0,4,3} + L^R_{0,1}L^R_{6,1}K^R_{0,4,6} + L^R_{0,2}K^R_{0,4,5} + L^R_{0,7}L^R_{4,7}K^R_{0,4,4}) & \text{x=1,y=1,i=0,j=4} \\
P_{in}(L^R_{0,1}L^R_{6,1}L_c^2K_c + L^R_{0,2}K_c) & \text{x=1, y=2, i=7, j=4} \\
P_{in}(K^R_{7,4,0} + L^R_{0,1}L^R_{6,1}K^R_{7,4,6} + L^R_{0,2}K^R_{7,4,5} + L^R_{0,7}L^R_{4,7}K^R_{7,4,4}) & \text{x=1,2p+1} \le \text{y} \le \text{N-3,i=7, j=4} \\
P_{in}(L^R_{0,6}L_c^4K_c + L^R_{0,2}K_c) & \text{x=1,2p+2} \le \text{y} \le \text{N-4,i=7, j=4} \\
P_{in}(L^R_{0,3}L^R_{8,3}L^R_{8,1}L^{R,3}_{6,1}L_c^2K_c + L^R_{0,3}L^R_{8,3}L^{R,2}_{8,2}L^{R,2}_{5,2}K_c) & \text{x=1, y=N-2, i=7, j=4} \\
P_{in}(K^R_{7,4,0} + L^R_{0,4}L^R_{7,4}L^R_{7,1}L^{R,3}_{6,1}K^R_{7,4,6} + L^R_{0,4}L^R_{7,4}L^{R,2}_{7,2}L^{R,2}_{5,2}K_{7,4,5} + L^R_{0,7}K^R_{7,4,4}) & \text{x=1, y=N-1, i=7, j=4} \\
P_{in}(K^R_{7,6,0} + L^R_{0,3}L^R_{8,3}K^R_{7,6,8} + L^R_{0,1}L^R_{6,1}K^R_{7,6,6} + L^R_{0,2}K^R_{7,6,5}) & \text{x=1, y=N, i=7, j=6} \\
P_{in}(L^R_{0,3}L^R_{8,3}L_c^2K_c + L^R_{0,4}K_c) & \text{x=2, y=N, i=1, j=6} \\
P_{in}(K^R_{1,6,0} + L^R_{0,3}L^R_{8,3}K^R_{1,6,8} + L^R_{0,4}K^R_{1,6,7} + L^R_{0,1}L^R_{6,1}K^R_{1,6,6}) & \text{2p+1} \le \text{x} \le \text{M-3,y=N,i=1, j=6} \\
P_{in}(L^R_{0,8}L_c^4K_c + L^R_{0,4}K_c) & \text{2p+2} \le \text{x} \le \text{M-4, y=N, i=1, j=6} \\
P_{in}(L^R_{0,3}L^R_{8,3}L_c^2K_c + L^R_{0,4}K_c) & \text{x=M-2, y=N, i=1, j=6} \\
P_{in}(K^R_{1,6,0} + L^R_{0,3}L^R_{8,3}K^R_{1,6,8} + L^R_{0,4}K^R_{1,6,7} + L^R_{0,1}K^R_{1,6,6}) & \text{x=M-1,y=N,i=1, j=6} \\
P_{in}(K^R_{1,0,0} + L^R_{0,3}L^R_{8,3}K^R_{1,0,8} + L^R_{0,4}K^R_{1,0,7} + L^R_{0,5}L^R_{2,5}K^R_{1,0,2}) & \text{x=M,y=N,i=1, j=0}
\end{cases}
$$

$$
N^R_{i,j_{(4th)}}(x,y,ws_{i,j}(x,y)) = \tag{35}
$$

$$
\begin{cases}
P_{in}(L^R_{0,5}K^R_{0,4,2} + L^R_{0,2}L^R_{5,2}K^R_{0,4,5} + L^R_{0,4}L^R_{7,4}K^R_{0,4,7} + L^R_{0,7}L^R_{4,7}K^R_{0,4,4}) & \text{x=2,y=3,i=0,j=4} \\
P_{in}(L^R_{0,1}L_c^2K_c + L^R_{0,5}L_c^2K_c) & \text{x=2, 2p+2} \le \text{y} \le \text{N-2, i=7, j=4} \\
P_{in}(K^R_{7,4,0} + L^R_{0,2}L^R_{5,2}K^R_{7,4,5} + L^R_{0,5}K^R_{7,4,2} + L^R_{0,7}L^R_{4,7}K^R_{7,4,4}) & \text{x=2,2p+3} \le \text{y} \le \text{N-5,i=7, j=4} \\
P_{in}(K^R_{7,4,0} + L^R_{0,4}L^R_{7,4}L^R_{7,2}L^{R,3}_{5,2}K^R_{7,4,5} + L^R_{0,7}L^R_{4,7}K^R_{7,4,4} + L^R_{0,5}K^R_{7,4,2}) & \text{x=2, y=N-3, i=7, j=4} \\
P_{in}(K^R_{7,5,0} + L^R_{0,2}L^R_{5,2}K^R_{7,5,5} + L^R_{0,7}K^R_{7,5,4} + L^R_{0,5}K^R_{7,5,2}) & \text{x=2, y=N-1, i=7, j=5} \\
P_{in}(L^R_{0,8}L_c^4K_c + L^R_{0,4}K_c) & \text{2p+1} \le \text{x} \le \text{M-3,y=N-1,i=2, j=5} \\
P_{in}(K^R_{2,5,0} + L^R_{0,4}L^R_{7,4}K^R_{2,5,7} + L^R_{0,7}K^R_{2,5,4} + L^R_{0,2}L^R_{5,2}K^R_{2,5,5}) & \text{2p+2} \le \text{x} \le \text{M-2, y=N-1, i=2, j=5} \\
P_{in}(L^R_{0,3}L_c^4K_c + L^R_{0,7}L_c^2K_c) & \text{x=M-1,y=N-1,i=2, j=5} \\
P_{in}(K^R_{2,0,0} + L^R_{0,4}L^R_{7,4}K^R_{2,0,7} + L^R_{0,7}K^R_{2,0,4} + L^R_{0,6}K^R_{2,0,1}) & \text{x=M,y=N-1,i=2, j=0}
\end{cases}
$$

$$
\begin{aligned}
&P_{N4} = b_1 + b_2 + b_3 \qquad (36)\\
&b_1 = L_{4,2}^{\frac{N}{2}-3}L_{4,3}L_{1,3}^{\frac{M}{2}-2}L_{1,0}L_c^{3M+3N-18}N_{0,2}(2,3)\\
&b_2 = L_{4,3}L_{1,3}^{\frac{M}{2}-2}L_{1,0}L_c^{3M-4}\left(\sum_{j=2p+2}^{N-2}L_{4,2}^{\lfloor\frac{N-2-j}{2}\rfloor}L_c^{6\lfloor\frac{N-2-j}{2}\rfloor}N_c(2,4)\right) +\\
&L_{4,3}L_{1,3}^{\frac{M}{2}-2}L_{1,0}L_c^{3M}\left(\sum_{j=2p+3}^{N-5}L_{4,2}^{\lfloor\frac{N-2-j}{2}\rfloor}L_c^{6\lfloor\frac{N-2-j}{2}\rfloor}N_{4,2}(2,5)\right)\\
&b_3 = L_{4,3}L_{1,3}^{\frac{M}{2}-2}L_{1,0}L_c^{3M}N_{4,2}(2,N-3) + L_{1,3}^{\frac{M}{2}-2}L_{1,0}L_c^{3M-6}N_{4,3}(2,N-1) +\\
&L_{1,0}L_c^2\left(\sum_{i=2p+1}^{M-3}L_{1,3}^{\lfloor\frac{M-1-i}{2}\rfloor}L_c^{6\lfloor\frac{M-1-i}{2}\rfloor}N_c(3,N-1)\right) + L_{1,0}L_c^6\left(\sum_{i=2p+2}^{M-2}L_{1,3}^{\lfloor\frac{M-1-i}{2}\rfloor}L_c^{6\lfloor\frac{M-1-i}{2}\rfloor}N_{1,3}(4,N-1)\right) +\\
&L_c^2L_{1,0}N_c(M-1,N-1) + N_{1,0}(M,N-1)
\end{aligned}
$$

APPENDIX

A. Example of Router Region Model

Fig. 17 depicts the router region 1, shown in Fig. 5, defined for the folded-torus-based ONoCs. Considering (12), the insertion losses for the router region 1 are calculated in (33). In this equation, for example, the insertion loss from the input port I^{ip}_{R0} toward the output port I^{op}_{R3} in the router region, $L^R_{0,3}(x,y)$, consists of the insertion loss caused by the

$$N^R_{i,j_{(5th)}}(x, y, ws_{i,j}(x, y)) = \tag{37}$$
$$\begin{cases} P_{in}(L^R_{0,5}K^R_{0,4,2} + L^R_{0,2}L^R_{5,2}K^R_{0,4,5} + L^R_{0,4}L^R_{7,4}K^R_{0,4,7} + L^R_{0,7}L^R_{4,7}K^R_{0,4,4}) & \text{x=2,y=5,i=0,j=4} \\ P_{in}(L^R_{0,1}L^2_cK_c + L^R_{0,5}L^2_cK_c) & \text{x=2,2p+4} \le \text{y} \le \text{N-2, i=7, j=4} \\ P_{in}(K^R_{7,4,0} + L^R_{0,2}L^R_{5,2}K^R_{7,4,5} + L^R_{0,5}K^R_{7,4,2} + L^R_{0,7}L^R_{4,7}K^R_{7,4,4}) & \text{x=2,2p+5} \le \text{y} \le \text{N-5,i=7, j=4} \\ P_{in}(K^R_{7,4,0} + L^R_{0,4}L^R_{7,4}L^R_{7,2}L^{R,3}_{5,2}K^R_{7,4,5} + L^R_{0,7}L^R_{4,7}K^R_{7,4,4} + L^R_{0,5}K^R_{7,4,2}) & \text{x=2, y=N-3, i=7, j=4} \\ P_{in}(K^R_{7,5,0} + L^R_{0,2}L^R_{5,2}K^R_{7,5,5} + L^R_{0,7}K^R_{7,5,4} + L^R_{0,5}K^R_{7,5,2}) & \text{x=2, y=N-1, i=7, j=5} \\ P_{in}(L^R_{0,8}L^4_cK_c + L^R_{0,4}K_c) & \text{2p+1} \le \text{x} \le \text{M-3,y=N-1,i=2, j=5} \\ P_{in}(K^R_{2,5,0} + L^R_{0,4}L^R_{7,4}K^R_{2,5,7} + L^R_{0,7}K^R_{2,5,4} + L^R_{0,2}L^R_{5,2}K^R_{2,5,5}) & \text{2p+2} \le \text{x} \le \text{M-2, y=N-1, i=2, j=5} \\ P_{in}(L^R_{0,3}L^4_cK_c + L^R_{0,7}L^2_cK_c) & \text{x=M-1,y=N-1,i=2, j=5} \\ P_{in}(K^R_{2,0,0} + L^R_{0,4}L^R_{7,4}K^R_{2,0,7} + L^R_{0,7}K^R_{2,0,4} + L^R_{0,6}K^R_{2,0,1}) & \text{x=M,y=N-1,i=2, j=0} \end{cases}$$

$$N_{X,j} = \begin{cases} P_{in}(L_{in,w}L^3_bL^2_{c0}L_{c1}L_{p1}K_c + L_{in,n}L^2_bL^2_cL_{c0}L_{p0}L_{p1}(K_{p0}L^2_c + K_c)(1 + L_bL^3_cL_{c0})) & j = 1 \\ P_{in}(L_{p0}(K_{p0}L^2_c + K_c)(L_{in,n}L_{p0}L^6_c + L_{in,s}L_{c0}L^{-D}_p)) & j = 3 \\ P_{in}(L_{p0}(K_{p0}L^2_c + K_c)(L_{in,e}L_{s,n}L_{w,n}L_{p0}L^{18}_c + L_{in,s}L_{c0}L^{-D}_p)) & j = N-1 \\ P_{in}(L_{in,e}(K_cL^2_{p0} + K_{p0})(L^2_c + \frac{1}{L^2_bL_cL_{c0}L_{p1}L^{-D}_p})) & \\ +P_{in}(L^2_c(K_{p0}L^2_c + K_c)(\frac{L_{in,e}L_{e,s}L_{w,n}}{L^2_{c0}L^{-2D}_p} + \frac{L_{in,n}L_{s,ej}L^4_cL_{c0}L_{c1}}{L^2_bL_{p0}})) & j = N \end{cases} \tag{39}$$

$$N_{C,X,j} = \begin{cases} P_{in}(L_{in,n}K_c(L_{s,n}L_bL^{10}_c + L^6_c + 1)) & j = 2 \\ P_{in}(K_c(L_{in,s}L^4_c + L_{in,n})) & j = 4 \\ P_{in}(K_c(L_{in,e}L_{w,n}L_bL^2_{s,n}L^{22}_c + L_{in,e}L_{w,n}L_{s,n}L^{18}_c + L_{in,n})) & j = N-2 \end{cases} \tag{40}$$

$$N_{Y,i} = \begin{cases} P_{in}(L_{in,e}L^4_c(K_cL^2_{p0} + K_{p0})(L^2_c + L_bL^4_{c0}) + L_{in,n}(\frac{K_cL^2_{p0}+K_{p0}}{L_cL_{c0}L_{c1}L^{-D}_p} + \frac{L_{s,ej}L_{n,s}L^6_cK_{p0}}{L^2_{p0}L^{-D}_p})) & i = 3 \\ P_{in}(L_{in,e}L^4_c(K_cL^2_{p0} + K_{p0})(L^2_c + L_bL^4_{c0}) + \frac{L_{in,n}(K_cL^2_{p0}+K_{p0})}{L_cL_{c0}L_{c1}L^{-D}_p} + \frac{L_{in,s}L_{s,ej}L_{n,s}L_bL^4_cK_{p0}}{L^2_{p0}L^{-D}_p}) & i = M-1 \\ P_{in}(L_{in,s}L^2_cK_{p0} + \frac{L_{in,e}L_{p0}K_c}{L_cL_{p1}L^{-D}_p} + L_{in,e}L^2_bL_{c0}L_{p0}(K_cL^2_{p0} + K_{p0})(L_b + L^7_cL_{c0})) & i = M \end{cases} \tag{41}$$

$$N_{C,Y,i} = \begin{cases} P_{in}(L_{in,e}K_c(L_{e,w}L_bL^8_c + 1)) & i = 2 \\ P_{in}(K_c(L_{in,w}L^4_c + L_{in,e})) & i = 4 \\ P_{in}(L_{in,e}K_c(L_{e,w}L^2_bL^8_c + L_{w,e}L_bL^{10}_c + L^6_c + 1)) & i = M-2 \end{cases} \tag{42}$$

optical router from the injection port to the west output port, $L_{0,4}(x, y)$, and a waveguide bending loss, L_b. The calculations for the other router regions follow the same principles.

B. Crosstalk Noise and SNR Analytical Equations

We present detailed analytical equations for calculating the crosstalk noise and SNR of different optical links that are among the longest. Utilizing (14) and Fig. 6(a), the crosstalk noise introduced at the router on the X-section and at the router region $R^2(x, N)$ on the Y-section of the longest link is calculated in (34), given on page 12. In this equation, $ws_{i,j}(x, y)$ is defined as the worst-case status of the optical router $R(x, y)$ while considering the statuses of the other optical routers to guarantee the worst-case crosstalk noise analyses. In this paper, $p \in \{1, 2, 3, \cdots\}$ in the equations. The crosstalk noise power, P_{N1}, and the SNR received at the destination of the longest optical link, defined in (19), can be calculated using (18) and (34). The same procedure can be used to analyze the SNR for the other three longest optical links shown in Fig. 6.

Following the same principles discussed for the longest optical link, the crosstalk noise introduced at the router regions on the X-section and Y-section of the second and third longest links can be calculated. Moreover, the crosstalk noise power, P_{N2} and P_{N3}, and the SNR received at the destination of these links can be described based on (20), (21) and the crosstalk noise accumulated at different optical routers on these links. Considering the next longest optical links, the crosstalk noise introduced at the router region $R^2(2, y)$ on the X-section and at the router regions $R^2(x, N-1)$ on the Y-section of the fourth and fifth longest optical links are calculated in (35) and (37), respectively, given on pages 12 and 13. Furthermore, the crosstalk noise power and the SNR received at the destination of these optical links can be calculated based on (36) for the fourth longest optical link, and (23) and (37) for the fifth longest optical link. In (36), the router region is expanded to the general router model.

Considering the SNR equation of the fourth longest optical link shown in (26) and the crosstalk noise power added to this link described in (36), the SNR equation of the fourth longest optical link can be represented as (38). This equation helps compare the SNR of the fourth and the fifth longest optical links. b_1, b_2, and b_3 are defined in (36)

$$SNR_{(2,3),(M,N-1)} = \frac{a}{b_1 + b_2 + b_3} \tag{38}$$
$$a = L_{0,2}L^{\frac{N}{2}-3}_{4,2}L_{4,3}L^{\frac{M}{2}-2}_{1,3}L_{1,0}L^{3M+3N-18}_c.$$

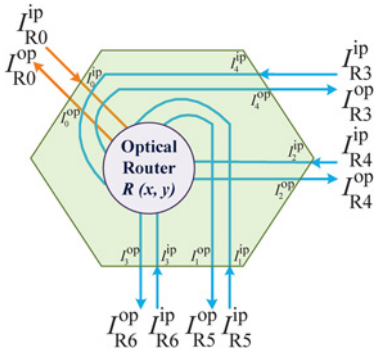

Fig. 17. Router region 1 defined for the folded-torus-based ONoCs.

Considering the folded-torus-based ONoCs using Crux optical router and Fig. 14(a), the crosstalk noise added at the optical router j on the X-section of the worst-case SNR link, N_X, is calculated in (39), given on page 14. Moreover, (40), given on page 14, calculates the crosstalk noise added at the network level, $N_{C,X}$, on the X-section of this link. The crosstalk noise introduced at the optical router i on the Y-section of the worst-case SNR link, N_Y, can be written as (41), given on page 14, while the crosstalk noise added at the network level, $N_{C,Y}$, is defined in (42), given on page 14. Moreover, the worst-case crosstalk noise power in folded-torus-based ONoCs using the Crux optical router can be defined based on (31), (39), (41), (40), and (42). The worst-case crosstalk noise and SNR in folded-torus-based ONoCs using the optimized crossbar optical router can be calculated similarly.

REFERENCES

[1] *International Technology Roadmap for Semiconductors (ITRS)* [Online]. Available: http://www.itrs.net
[2] A. Rahman and R. Reif, "System-level performance evaluation of 3-D integrated circuits," *IEEE Trans. Very Large Scale Integr. (VLSI) Syst.*, vol. 8, no. 6, pp. 671–678, Dec. 2000.
[3] S. J. Souri, K. Banerjee, A. Mehrotra, and K. Saraswat, "Multiple Si layer ICs: Motivation, performance analysis, and design implications," in *Proc. IEEE/ACM Design Autom. Conf.*, 2000, pp. 213–220.
[4] V. Chan, K. Hall, E. Modiano, and K. Rauschenbach, "Architectures and technologies for high-speed optical data networks," *J. Lightw. Technol.*, vol. 16, no. 12, pp. 2146–2168, Dec. 1998.
[5] M. M. Vaez and C. T. Lea, "Strictly nonblocking directional-coupler-based switching networks under crosstalk constraint," *IEEE Trans. Commun.*, vol. 48, no. 2, pp. 316–323, Feb. 2000.
[6] Y. Xie, M. Nikdast, *et al.*, "Crosstalk noise and bit error rate analysis for optical network-on-chip," in *Proc. ACM/IEEE Design Autom. Conf.*, Jun. 2010, pp. 657–660.
[7] H. Chen and A. W. Poon, "Low-loss multimode-interference-based crossings for silicon wire waveguides," *IEEE Photon. Technol. Lett.*, vol. 18, no. 21, pp. 2260–2262, Nov. 2006.
[8] C. H. Chen and C. H. Chiu, "Taper-integrated multimode-interference based waveguide crossing design," *IEEE J. Quantum Electron.*, vol. 46, no. 11, pp. 1656–1661, Nov. 2010.
[9] X. Li, F. Ou, Z. Hou, Y. Huang, and S.-T. Ho, "Experimental demonstration and simulation of lossless metal-free integrated elliptical reflectors for waveguide turnings and crossings," in *Proc. CLEO*, May 2011, pp. 1–2.
[10] W. Ding, D. Tang, Y. Liu, L. Chen, and X. Sun, "Compact and low crosstalk waveguide crossing using impedance matched metamaterial," *Appl. Phys. Lett.*, vol. 96, no. 11, pp. 111114-1–111114-3, Mar. 2010.
[11] Y. Xie, M. Nikdast, J. Xu, X. Wu, W. Zhang, Y. Ye, *et al.*, "Formal worst-case analysis of crosstalk noise in mesh-based optical networks-on-chip," *IEEE Trans. Very Large Scale Integr. (VLSI) Syst.*, vol. 21, no. 10, pp. 1823–1836, 2013.
[12] J. Chan, G. Hendry, K. Bergman, and L. Carloni, "Physical-layer modeling and system-level design of chip-scale photonic interconnection networks," *IEEE Trans. Computer-Aided Design Integr. Circuits Syst.*, vol. 30, no. 10, pp. 1507–1520, Oct. 2011.
[13] D. Ding, B. Yu, and D. Z. Pan, "GLOW: A global router for low-power thermal-reliable interconnect synthesis using photonic wavelength multiplexing," in *Proc. ASPDAC*, 2012, pp. 621–626.
[14] N. Sherwood-droz, K. Preston, J. S. Levy, and M. Lipson, "Device guidelines for WDM interconnects using silicon microring resonators," in *Proc. WINDS*, 2010, pp. 20–22.
[15] B. C. Lin and C. T. Lea, "Crosstalk analysis for microring based optical interconnection networks," *J. Lightw. Technol.*, vol. 30, no. 15, pp. 2415–2420, 2012.
[16] Y. Ye, J. Xu, X. Wu, W. Zhang, W. Liu, and M. Nikdast, "A torus-based hierarchical optical-electronic network-on-chip for multiprocessor system-on-chip," *J. Emerg. Technol. Comput. Syst.*, vol. 8, no. 1, pp. 1–26, Feb. 2012.
[17] F. Xia, L. Sekaric, and Y. Vlasov, "Ultracompact optical buffers on a silicon chip," *Nature Photon.*, vol. 1, no. 1, pp. 65–71, 2007.
[18] G. R. Zhou, X. Li, and N. N. Feng, "Design of deeply etched antireflective waveguide terminators," *IEEE J. Quantum Electron.*, vol. 39, no. 2, pp. 384–391, Feb. 2003.
[19] M. Nikdast, J. Xu, *et al.*, (2013). *Crosstalk Noise and Loss Analysis Platform (CLAP)* [Online]. Available: http://www.ust.hk/~eexu
[20] P. Dong, W. Qian, *et al.*, "Low loss silicon waveguides for application of optical interconnects," *Proc.IEEE Photonics Soc. Summer Topical Meeting Series*, pp. 191–192, Nov. 2010.

Mahdi Nikdast (S'10) was born in Esfahan, Iran, in 1987. He received the B.Sc. degree in computer engineering (Hons.) from Islamic Azad University, Esfahan, in 2009. Since 2009, he has been pursuing the Ph.D. degree at the Department of Electronic and Computer Engineering, Hong Kong University of Science and Technology (HKUST), Clear Water Bay, Hong Kong.

He is currently involved in SNR analyses for ONoCs with the Mobile Computing System Laboratory, Department of Electronic and Computer Engineering, HKUST. His current research interests include embedded and computing systems, multiprocessor systems-on-chip, networks-on-chip, and optical interconnection networks.

Mr. Nikdast was a recipient of the Second Best Project Award at the 6th Annual AMD Technical Forum and Exhibition in 2010.

Jiang Xu (S'02–M'07) received the Ph.D. degree from Princeton University, Princeton, NJ, USA, in 2007.

From 2001 to 2002, he was with Bell Laboratories, Murray Hill, NJ, USA, as a Research Associate. He was a Research Associate with NEC Laboratories America, Princeton, NJ, USA, from 2003 to 2005. He joined a startup company, Sandbridge Technologies, Tarrytown, NY, USA, from 2005 to 2007, and developed, as well as implemented, two generations of NoC-based ultralow power multiprocessor systems-on-chip for mobile platforms. He is currently an Associate Professor with the Hong Kong University of Science and Technology, Clear Water Bay, Hong Kong. He is the Founding Director of the Xilinx-HKUST Joint Laboratory and establishes the Mobile Computing System Laboratory. He has authored and co-authored more than 70 book chapters and papers in peer-reviewed journals and international conferences. His current research interests include networks-on-chip, multiprocessor systems-on-chip, embedded systems, computer architectures, low-power very large scale integration design, and HW/SW codesign.

Dr. Xu currently serves as an Associate Editor of the *ACM Transactions on Embedded Computing Systems* and the IEEE TRANSACTIONS ON VERY LARGE SCALE INTEGRATION SYSTEMS. He is an ACM Distinguished Speaker and a Distinguished Visitor of the IEEE Computer Society. He served on the steering committees, organizing committees, and technical program committees of many international conferences.